

Travelling Waves Solutions of Cell-Invasion Driven by a Velocity
Jump Process

Brody Foy

January 25, 2013

Contents

1	Introduction	1
2	The Initial Model	2
3	Travelling Wave Analysis	4
3.1	Case 1: No Turning, $\Lambda = 0$	4
3.2	Case 2: Dominant Turning, $\Lambda \rightarrow \infty$	4
3.3	Case 3: Intermediate Turning	7
4	Conclusion	9
4.1	Acknowledgements	9

Abstract

Cell invasion is a biological process characterised by the movement of a cell front(s) into previously unoccupied territory. It is essential in many different areas, including wound repair and disease development. Traditionally, mathematical models of cell-invasion are based on the classical Fisher-Kolmogorov equation. These generally lead to the models being parabolic in nature. While this is acceptable in some circumstances, it means the model cannot represent experimental measurements of individual cells as it implies that information propagates forward with infinite speed. To overcome this limitation, a new style model of cell-invasion was studied which is built up from a velocity-jump process in which information propagates with finite speed. This model is 1-D, breaking the cells into two subpopulations; a left-moving $L(x, t)$ and a right moving $R(x, t)$. This leads to the creation of a coupled system of hyperbolic partial differential equations. This system was then analysed and solved numerically (and analytically in special cases) for a wide-variety of parameter choices. In doing this a variety of different behaviours could be seen, including the transition from smooth monotone travelling wave solutions to smooth non-monotone travelling wave solutions. The research was concluded by considering the appropriateness of the model, as well as possible future extensions to it.

Section I

Introduction

Cell invasion is an extremely important biological process. It is characterised by the movement of a 'front' or 'wall' of cells into a previously unoccupied area [5, 6]. This behaviour can be readily found in many biological systems, including in wound healing, tissue repair and disease development. Often these fronts arise in cell populations that are motile and proliferate up to a carrying capacity. This is because as these two processes combine, they lead to forward motion of cells which proliferate fast enough to leave full density behind them.

Most traditional models of cell-invasion are based on the Fisher-Kolmogorov equation [2, 3] in some way. Due to the nature of this equation, the subsequent models are normally parabolic reaction-diffusion style equations, which support travelling wave solutions [2]. A more recent version of cell invasion modelling involves the creation of discrete position-jump models, trying to account for behaviour of individual cells, and then transform the discrete equations into continuum style models.

Due to many recent advances in microscopy and imaging, experimental measurements of many cell behaviours (including invasion) are becoming detailed enough to measure individual cell speeds [1, 4]. However, traditional models that are based on the Fisher-Kolmogorov equation cannot be used to make predictions about the speed of individual cells, as they are parabolic and subsequently imply that information propagates forward with infinite speed.

In order to overcome this limitation, we consider a continuum partial differential equation model built from a discrete random walk process known as a velocity-jump process. This newer style of modelling incorporates the fact that information propagates forward with finite speed, thus making it more biologically reasonable. Briefly, the discrete process (in one-dimension) involves breaking the total cell population into two subpopulations; a left-moving one, and a right moving one. Discretely, each cell can be thought to occupy one grid space on a lattice, with grid-length δ . During a given discrete time interval (duration τ) each cell agent can move a distance of $v\tau$ with probability P_m , where v is the cell velocity. This means that right-moving cells attempt to step a distance of $+v\tau$ and left-moving cells attempt to step a distance of $-v\tau$. Equally at any given time interval, an agent can change direction with probability P_t . In this way a left-moving cell can change to a right-moving cell and vice versa. Setting that $P_t = 0$ generates motion that is purely ballistic, setting $P_t \ll 1$ gives persistent motion, with only small levels of cell turning, while setting $1 - P_t \ll 1$ gives motion that is essentially persistence-free. Finally, at any time step an agent can proliferate, producing a daughter agent with probability P_p [7, 8].

Traditional velocity-jump models do not account for crowding effects. In effect the model assumes that multiple agents can reside at the same location in space and time and that agents can move through each other. This is of course biologically unreasonable, as cells have a finite size and thus cannot occupy the same location or move through each other. Motivated by this, a velocity-jump model was created that incorporated crowding effects so that each lattice site had a maximum occupancy of 1. The motility and proliferation mechanisms were also adapted so that any event that would cause a lattice site to surpass maximum occupancy was aborted. Beyond this it was shown that the resulting model was quite different to the usual models that arise from noninteracting velocity-jump processes that do not include crowding effects. In particular the work showed that the pde description of a proliferative velocity-jump process with crowding effects gives rise to moving cell fronts that are travelling wave solutions of the governing equations of the discrete processes [7].

The central aim of this report is to describe the travelling wave solutions of a new set of partial differential equations (pde) that can be used to describe cell motion. The travelling wave behaviours of this system are presented for three different cases: (i) Case 1, no turning (ii) Case 2, fast turning, and (iii) Case 3, intermediate turning. The system of pdes is solved using a combination of exact and numerical methods, and a range of travelling wave solutions are seen. These include transitions from smooth monotone wave behaviour to smooth nonmonotone behaviour. The solutions are also compared to the corresponding phase plane trajectories. Overall this leads to the conclusion that low turning rates are the most biologically relevant.

Section II

The Initial Model

Previous work [7] considered a discrete velocity-jump model of cell invasion with proliferation and crowding effects. By considering the discrete processes in one dimension, the following pde system is arrived at:

$$\begin{aligned}\frac{\partial R}{\partial t'} &= -v \frac{\partial}{\partial x'} [R(1 - S)] + \lambda(L - R) + \theta R(1 - S), \\ \frac{\partial L}{\partial t'} &= +v \frac{\partial}{\partial x'} [L(1 - S)] + \lambda(R - L) + \theta L(1 - S)\end{aligned}$$

Where $L(x', t')$, $R(x', t')$ and $S(x', t')$ are the left-moving, right-moving and total cell densities at point x' and time t' . The parameters are the cell velocity v , the turning force λ and the proliferation rate θ . All of these are related to the discrete process probabilities P_m , P_t and P_p .

Before analysis, the above system can be simplified by nondimensionalising. New spatial and temporal coordinates $t = t'/\theta$ and $x = vx'/\theta$ are introduced, leading to the system:

$$\begin{aligned}\frac{\partial R}{\partial t} &= -\frac{\partial}{\partial x'} [R(1 - S)] + \Lambda(L - R) + R(1 - S), \\ \frac{\partial L}{\partial t} &= +v \frac{\partial}{\partial x'} [L(1 - S)] + \Lambda(R - L) + L(1 - S).\end{aligned}$$

Where Λ is λ/θ , the ratio between the turning force and proliferation rate.

To fall in line with experimental observations (e.g. a scrape wound assay), these equations would need to operate on a finite domain with a heaviside style initial condition representing a section of the domain being at full density ($S(x, 0) = 1$), and the rest being empty ($S(x, 0) = 0$). However, to consider travelling wave solutions an infinite domain $-\infty < x < \infty$ is more appropriate. Equally, instead of a heaviside style function, we use an initial condition of the form:

$$L(x, 0) \equiv 0, \quad R(x, 0) = \begin{cases} 1, & x < 0 \\ \exp(-\xi x) & x \geq 0 \end{cases}$$

Where $\xi > 0$ is a constant. For appropriate large ξ this represents a fast transition between full density and no density, as the exponential decays quickly.

To analyse the travelling wave solutions of this pde, the transition needs to be made into a travelling wave coordinate. This is done by transforming the pde system of x and t into an ode of the new variable z through the substitution $z = x - ct$, where c is the wavespeed. Making this substitution leads to the system:

$$\begin{aligned}-c \frac{dR}{dz} &= -\frac{d}{dz} [R(1 - S)] + \Lambda(L - R) + R(1 - S), \\ -c \frac{dL}{dz} &= +\frac{d}{dz} [L(1 - S)] + \Lambda(R - L) + L(1 - S).\end{aligned}$$

For travelling wave solutions to exist for this system, there has to be a heteroclinic orbit between at least two of the system's steady states. These steady states can be found by expanding out the above equations and then setting $\frac{dL}{dz} = \frac{dR}{dz} = 0$. Doing this reveals that the system has two steady states:

$$(L, R) = (0, 0), \left(\frac{1}{2}, \frac{1}{2}\right).$$

To work out whether a heteroclinic orbit exists between these two steady states, phase plane analysis can be performed. By linearising around the first steady state, the eigenvalues of the Jacobian can be found to be:

$$\left(\frac{1}{2}, \frac{1}{2}\right) : \quad \mu_{1,2} = \frac{1}{c}, \frac{2\Lambda}{c}.$$

c and Λ are both positive parameters, and thus this steady state is an unstable node. For the second steady state the eigenvalues are:

$$(0, 0) : \quad \mu_{3,4} = \frac{c(\Lambda - 1) \pm \sqrt{c^2\Lambda^2 - 2\Lambda + 1}}{c^2 - 1}.$$

The nature of $\mu_{3,4}$ are much harder to see. However, through analysis it can be shown that as long as $c > 1$, the state is either a stable node, or a saddle point, both of which can draw at least one trajectory in. This means that a heteroclinic orbit exists such that solutions will travel out from $(\frac{1}{2}, \frac{1}{2})$ towards $(0, 0)$. This would correspond to a wave of cells moving from full split-density ($L = \frac{1}{2}, R = \frac{1}{2}$) towards the uninvaded territory ($L = 0, R = 0$).

As $x \rightarrow \infty$, the trajectory between the steady states would be expected to approach $(0, 0)$ along the most negative eigenvalue, such that:

$$R(z) \sim \exp(\mu_4 z)$$

This can be matched with the initial condition, to create the dispersion relationship:

$$c = \frac{1 - \Lambda + \sqrt{\Lambda^2 + \xi^2}}{\xi}.$$

This equation allows the wave speed to be directly controlled by specifically choosing the initial condition, which is key for analysing the system.

Section III

Travelling Wave Analysis

To simplify analysis of the system, results were split into three different cases corresponding to different Λ values. For each case a series of numerical results were generated, alongside (where possible) analytical results. Numerically the pdes were solved using an upwind finite different scheme on a uniform grid (with a grid spacing δx . A forward Euler Method (with constant step size δt) was used for the temporal integration.

The phase-planes presented were created from the ode system. The numerical trajectories were obtained using a fourth order Runge-Kutta method with a fixed step size δz .

3.1 Case 1: No Turning, $\Lambda = 0$

The first case presented is for when there is no turning. This means that $\lambda = 0$ and so consequently $\Lambda = 0$. With no turning, and an initial condition of $L(x, 0) = 0$, we can gather that $L(x, t) = 0$. This means that $S = R$ and the ode system becomes:

$$-c \frac{dR}{dz} = -\frac{d}{dz} [R(1 - R)] + R(1 - R).$$

This equation has the exact solution:

$$\frac{R(z)}{(1 - R(z))^{\frac{c+1}{c-1}}} = A \exp \left[-\frac{z}{c-1} \right],$$

where A is a constant of integration.

The set of pdes can be solved numerically, and overlaid against the analytical solution. The results of this can be seen in figures 3.1, 3.2 and 3.3. These figures show that the two solutions are very close, giving strength to the numerical results. The figures were generated with equal time spacings of 20, thus as c is increased the waves spread further apart. Equally it can be seen that as c increases the waves become more shallow.

3.2 Case 2: Dominant Turning, $\Lambda \rightarrow \infty$

The second case presented is for when $\Lambda \rightarrow \infty$. This corresponds to the turning force (λ) overpowering proliferation (θ) and becoming the most dominant dynamic in the system. If every cell is constantly trying to turn, it would be expected that over long time $L \rightarrow R$, and thus that $S \rightarrow 2R$. This once again turns the ode system into a singular equation:

$$-c \frac{dR}{dz} = R(1 - 2R).$$

As in the previous case, this can be solved to give an analytical form for $R(z)$

$$R(z) = \frac{A}{2A + \exp \left[\frac{z}{c} \right]},$$

where A is a constant of integration.

The set of pdes can be solved numerically and overlaid against the analytical solution. It should be noted that for the numerical results $\Lambda = 10$ was used to approximate $\Lambda \rightarrow \infty$, as even this reasonably small value was seen to be accurate against the analytical solution. The results of the numerical and analytical overlay can be seen in figures 3.4, 3.5 and 3.6. These figures show that the two solutions are very close, giving strength to the numerical results. The figures were generated with equal time spacings of 20, thus as c is increased the waves spread further apart. Equally it can be seen that as c increases the waves become more shallow. One of the key differences that can be seen between this case and the first case is that the waves are travelling out from 0.5 instead of 1. This is because there is now a left-moving population, thus at the waves back end the density should be evenly split and add to unity.

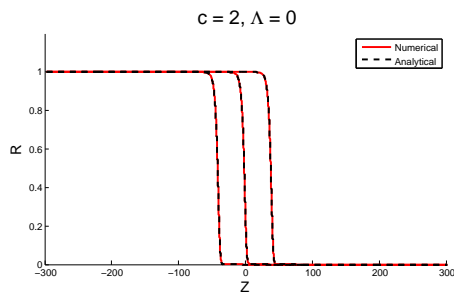


Figure 3.1: Plot of case 1, $\Lambda = 0, c = 2$, with 3 waves plotted at time spacings of 20

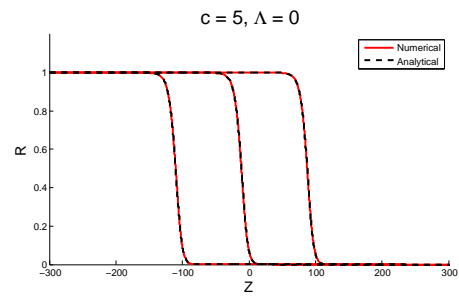


Figure 3.2: Plot of case 1, $\Lambda = 0, c = 5$, with 3 waves plotted at time spacings of 20

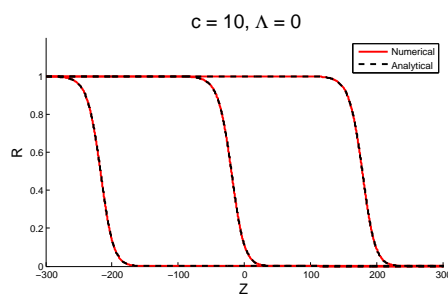


Figure 3.3: Plot of case 1, $\Lambda = 0, c = 10$, with 3 waves plotted at time spacings of 20

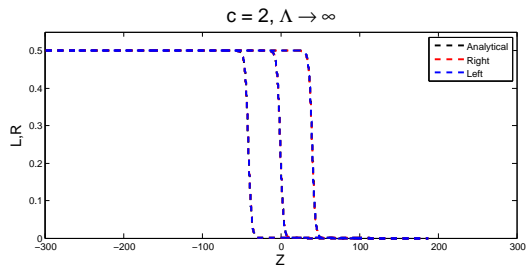


Figure 3.4: Plot of case 2, $\Lambda \rightarrow \infty, c = 2$, with 3 waves plotted at time spacings of 20

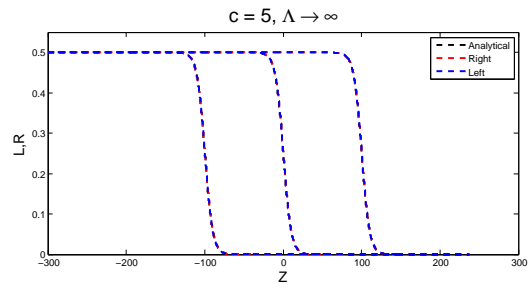


Figure 3.5: Plot of case 2, $\Lambda \rightarrow \infty, c = 5$, with 3 waves plotted at time spacings of 20

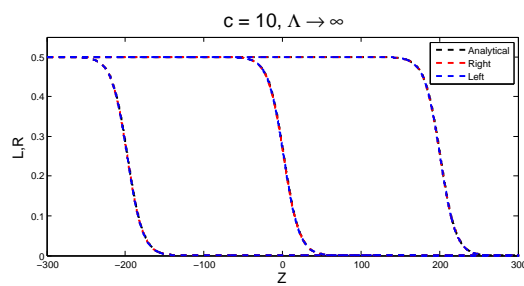


Figure 3.6: Plot of case 2, $\Lambda \rightarrow \infty, c = 10$, with 3 waves plotted at time spacings of 20

3.3 Case 3: Intermediate Turning

The third and final case presented is that of intermediate turning. In this case, the ode system cannot be separated or reduced to a singular equation and thus cannot be solved analytically. Therefore to compare the behaviour the solutions were gathered both through numerically solving the pde system and through creating a phase-plane of the ode system. This was done for three different 'intermediate' Λ values.

As can be seen in figures 3.7 and 3.8, low Λ values produce very non-monotone yet still smooth travelling waves. At the leading edge, the waves formed are extremely right dominant. Beyond this, key components of the numerical results can be seen in the behaviour of the phase-plane. The L and R values at the peak in R correspond accurately to where the right null-cline cuts the wave trajectory. Equally, the trajectory can be seen to push up into the Right plane initially, before pulling in towards $(0, 0)$. This matches up with the numerical results showing right dominance at the leading edge.

As Λ increases, the waves start to become more monotone. This can be seen in figures 3.9 and 3.10. The increase in Λ has flattened the wave trajectory significantly. This in turn has caused it to intersect the right null-cline at a much lower point, leading to a less pronounced peak in the right wave and less leading edge dominance.

As Λ increases once more the waves become fully monotone, although not fully overlaid. This can be seen in figures 3.11 and 3.12. This time in the phase-plane the trajectory has flattened much more, and subsequently does not appear to cut the right null-cline at all. This overall means that there is no peak in the right wave, making it monotone.

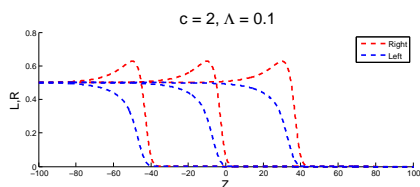


Figure 3.7: Plot of case 3, $\Lambda = 0.1, c = 2$, with 3 waves plotted at time spacings of 20

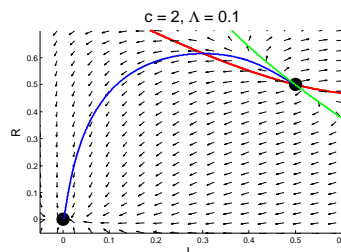


Figure 3.8: Phase Plane for case 3, $\Lambda = 0.1, c = 2$, showing the left null-cline (green), right null-cline (red), and wave trajectory (blue) between the two steady states (black dots)

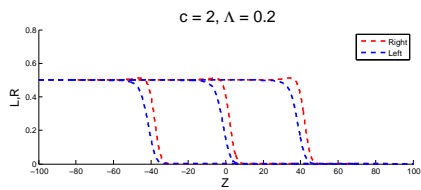


Figure 3.9: Plot of case 3, $\Lambda = 0.2, c = 2$, with 3 waves plotted at time spacings of 20

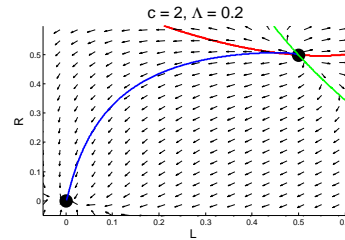


Figure 3.10: Phase Plane for case 3, $\Lambda = 0.2, c = 2$, showing the left null-cline (green), right null-cline (red), and wave trajectory (blue) between the two steady states (black dots)

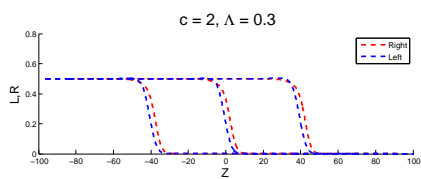


Figure 3.11: Plot of case 3, $\Lambda = 0.3, c = 2$, with 3 waves plotted at time spacings of 20

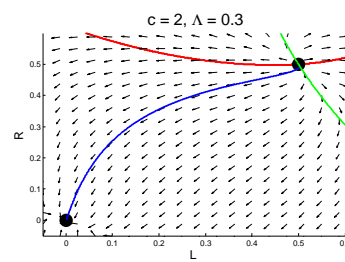


Figure 3.12: Phase Plane for case 3, $\Lambda = 0.3, c = 2$, showing the left null-cline (green), right null-cline (red), and wave trajectory (blue) between the two steady states (black dots)

Section IV

Conclusion

In biological wound healing, a cell front exists at the edge of the wound. As time progresses, this front invades the unhealed territory leaving full density healed cells behind it. This is a strong example of biological travelling wave behaviour. In wounds, as the healing progresses, it shows dominance in inwards motion. As the model analysis performed previously shows, this corresponds to a low Λ value meaning the turning force (λ) is not as dominant as proliferation (θ). Thus, a low Λ value appears to be the most biologically relevant choice for the model.

For further research, the model could be extended in many different ways. Firstly, it could be extended into higher dimensions through modifying the original velocity-jump process to account for 2-dimensional motion. Equally, it could be modified to account for other dynamics beyond proliferation and turning.

4.1 Acknowledgements

I would personally like to thank both AMSI and CSIRO for hosting the Big Day In Conference, as well as for providing a summer research scholarship. Equally, I would like to thank my two supervisors, Doctor Mat Simpson and Associate Professor Scott McCue for their help and guidance throughout the project.

Bibliography

- [1] Britto JM, Tait KJ, Johnston LA, Hammond VE, Kalloniatis M, Tan, SS. Altered speeds and trajectories of neurons migrating in the ventricular and subventricular zones of the reeler neocortex. *Cerebral Cortex*. 21 (2011) 1018.
- [2] Fisher RA. The wave of advance of advantageous genes. *Annals of Eugenics*. 7 (1937) 353.
- [3] Kolmogorov A, Petrovsky I, Piscounov N. Étude de léquation de la diffusion avec croissance de la quantité de matière et son application á un problème biologique. *Moscow University Bulletin of Mathematics*. 1 (1937) 1.
- [4] Kulesa PM, Teddy JM, Stark DA, Smith SE, McLennan R. Neural crest invasion is a spatially-ordered progression into the head with higher cell proliferation at the migratory front as revealed by the photoactivatable protein, KikGR. *Developmental Biology*. 315 (2008) 275.
- [5] Maini PK, McElwain DLS, Leavesley DI. Traveling wave model to interpret a wound-healing cell migration assay for human peritoneal mesothelial cells. *Tissue Engineering*. 10 (2004) 475.
- [6] Maini PK, McElwain DLS. Leavesley DI. Travelling Waves in a Wound Healing Assay. *Applied Mathematics Letters*. 17 (2004) 575.
- [7] Treloar KK, Simpson MJ, McCue SW. Velocity–jump models with crowding effects. *Physical Review E*. 84 (2011) 061920.
- [8] Treloar KK, Simpson MJ, McCue SW. Velocity–jump processes with proliferation. *Journal of Physics A: Mathematical and Theoretical*. 46 (2013) 015003.